British Journal of Pharmacology

DOI:10.1111/bph.12819
www.brjpharmacol.org

RESEARCH PAPER

Small-molecule modulators of the OX40–OX40 ligand co-stimulatory protein–protein interaction

Yun Song[1], Emilio Margolles-Clark[2], Allison Bayer[3,4] and Peter Buchwald[1,3]

[1]*Department of Molecular and Cellular Pharmacology, University of Miami, Miami, FL, USA,* [2]*Department of Surgery, Division of Transplants, University of Miami, Miami, FL, USA,* [3]*Diabetes Research Institute, University of Miami, Miami, FL, USA, and* [4]*Department of Microbiology and Immunology, Miller School of Medicine, University of Miami, Miami, FL, USA*

Correspondence
Peter Buchwald, Diabetes Research Institute, Miller School of Medicine, University of Miami, 1450 NW 10 Ave (R-134), Miami, FL 33136, USA. E-mail: pbuchwald@med.miami.edu

Received
16 December 2013
Revised
22 April 2014
Accepted
7 June 2014

BACKGROUND AND PURPOSE

The OX40–OX40L protein–protein interaction (PPI) is an important cell-surface signalling co-stimulatory regulator within the TNFR superfamily (TNFRSF) and a promising therapeutic target for immunomodulation. PPIs are difficult to modulate using small-molecules. Here, we describe the identification of a small-molecule OX40 modulator and confirm its partial agonist character.

EXPERIMENTAL APPROACH

Cell-free screening assays were developed and used to identify OX40–OX40L inhibitors. Modified versions of this assay were used to elucidate the binding partner and the binding nature of active compounds. OX40-transfected sensor cells with NF-κB reporters were constructed and used to confirm and characterize activity and specificity. Immunomodulatory activity and partial agonist nature were further confirmed by *ex vivo* T-cell polarization assays.

KEY RESULTS

Several compounds that concentration-dependently affected OX40-OX40L were identified. Cell assays indicated that they were partial agonists with low micromolar potency and adequate selectivity. Under polarizing conditions based on TGF-β, the most promising compound mimicked the effect of an agonistic anti-OX40 antibody in suppressing regulatory T-cell generation and diverting $CD4^+CD62L^+Foxp3^-$ cells to T_H9 phenotype *in vitro*.

CONCLUSIONS AND IMPLICATIONS

We identified, to our knowledge, the first small-molecule compounds able to interfere with OX40–OX40L binding and, more importantly, to act as partial agonists of OX40. This is particularly interesting, as small-molecule agonism or activation of PPIs is considered unusually challenging and there are only few known examples. These results provide proof-of-principle evidence for the feasibility of small-molecule modulation of the OX40–OX40L interaction and for the existence of partial agonists for TNFRSF-PPIs.

Abbreviations

BrdU, bromodeoxyuridine (5-bromo-2′-deoxyuridine); CVN, chlorazol violet N; OX40L, OX40 ligand (also known as TNFSF4); PPI, protein–protein interaction; SEAP, secreted embryonic alkaline phosphatase; T1D, type 1 diabetes; TNFRSF, tumour necrosis factor receptor superfamily

Table of Links

TARGETS	LIGANDS
OX40 (TNFRSF4)	OX40L
CD40 (TNFRSF5)	CD40L
RANK (TNFRSF11A)	RANKL
4-1BB (TNFRSF9)	4-1BBL
TNFR1 (TNFRSF1A)	TNF-α
	TGF-β1
	IL-2
	IL-4

This Table lists key protein targets and ligands in this document, which are hyperlinked to corresponding entries in http://www.guidetopharmacology.org, the common portal for data from the IUPHAR/BPS Guide to PHARMACOLOGY (Pawson *et al.*, 2014) and are permanently archived in the Concise Guide to PHARMACOLOGY 2013/14 (Alexander *et al.*, 2013).

Introduction

OX40 (ACT35, CD134, TNFRSF4), a surface type 1 transmembrane glycoprotein expressed on a variety of cell types, is one of the most important and widely studied members of the TNF receptor superfamily (TNFRSF). The biological and pathological responses initiated upon OX40 ligand (OX40L, CD252, CD134L, gp34, TNFSF4) binding have been thoroughly studied, and modulation of the OX40–OX40L co-stimulatory interaction is a particularly promising therapeutic target for immunomodulation (Sugamura *et al.*, 2004; Croft *et al.*, 2009; Croft, 2010; Ishii *et al.*, 2010). Either inhibition or stimulation of OX40 signalling could be beneficial depending on the nature of the physiological and pathological conditions targeted, and biological drugs targeting this pathway are in clinical trials for asthma and prostate cancer respectively (Tansey and Szymkowski, 2009; Sheridan, 2013; Yao *et al.*, 2013). Of particular interest, inhibition of the OX40–OX40L co-stimulatory interaction at week 12 has been shown to significantly reduce the incidence of autoimmune diabetes in NOD mice, a common animal model of type 1 diabetes (T1D) (Pakala *et al.*, 2004). OX40 has also been shown to be involved in controlling allograft tolerance (Kinnear *et al.*, 2013), including islet allograft tolerance (Chen *et al.*, 2008). In contrast, the positive modulation of OX40 expressed on both $CD4^+$ and $CD8^+$ T-cells could lead to promising immunostimulatory candidates for tumour therapy (Kjaergaard *et al.*, 2000; Weinberg *et al.*, 2000; Piconese *et al.*, 2008) or as antigen-specific adjuvants in T1D (Bresson *et al.*, 2011). Augmentation of anti-tumour T-cell effector activity or suppression of regulatory T-cell function has been observed on injection of agonistic OX40 antibodies (OX86), OX40L-Ig fusion proteins and RNA aptamers that bind OX40 in many animal models (Weinberg *et al.*, 2000; Dollins *et al.*, 2008; Piconese *et al.*, 2008). Recently, OX86 has also been shown to synergize with the antigen-specific prevention of T1D *in vivo* in NOD mice (Bresson *et al.*, 2011). Thus, small-molecule agonists or antagonists of OX40 could become not only valuable tools for studying the immunomodulatory role of this interaction but also potential therapeutics of interest for tumour suppression or immune diseases, including T1D and other autoimmune disorders.

The OX40–OX40L interaction is a typical protein–protein interaction (PPI) that, along with all other PPIs, was considered undruggable by small molecules for a long time because the relatively large protein interfaces involved in these interactions generally lack well-defined binding pockets as compared to most of the traditional targets such as enzymes or GPCRs (Hopkins and Groom, 2002; Smith *et al.*, 2006; Cheng *et al.*, 2007). Nevertheless, within the last few years, several sufficiently effective and even clinically promising small-molecule PPI inhibitors (PPIIs) have been identified for a number of different targets (Cochran, 2000; Arkin and Wells, 2004; Whitty and Kumaravel, 2006; Wells and McClendon, 2007; Buchwald, 2010). By focusing on the chemical space of organic dyes, we have recently identified the first small-molecule inhibitors of the CD40–CD40L co-stimulatory PPI (Margolles-Clark *et al.*, 2009a,b) as well as what seem to be the first promiscuous small-molecule PPIIs (Ganesan *et al.*, 2011). By all accounts, the identification of small-molecule PPI stimulators is even more challenging than that of PPI inhibitors since they, in addition to binding, also need to trigger the downstream activation cascade. Only a very limited number of small-molecule PPI 'agonists' (i.e., enhancers or stabilizers) have been identified to date; published examples include stabilizers of some of the PPIs in which protein 14-3-3 is involved (Rose *et al.*, 2010; Milroy *et al.*, 2013; Ottmann, 2013) and a possible small-molecule activator of the TNF-related apoptosis-inducing ligand receptor DR5 (also known as TNFRSF10B; Wang *et al.*, 2013).

Here, we report results of our ongoing search for small-molecule co-stimulatory modulators focusing on the OX40–OX40L interaction. We have identified several compounds with relatively well-defined structural scaffolds capable of interfering with the OX40–OX40L PPI with low micromolar potency in cell-free screening assays. Notably, subsequent cell-based assays revealed that several of them are capable of stimulatory activity at OX40 and mechanistic studies indicated that they act as partial agonists.

Methods

PPI binding assays

Microtitre plates (Nunc FMaxisorp; 96-well) were coated overnight at 4°C with 100 µL per well of Fc-conjugated receptors diluted in PBS 7.2. This was followed by blocking with 200 µL per well of blocking solution (PBS 7.2, 0.05% Tween-20, 1% BSA) for 1 h at room temperature (RT). Then, plates were washed twice using washing solution (PBS 7.4, 0.05% Tween-20) and tapped dry before the addition of the appropriate FLAG-tagged/biotinylated ligands along with different concentrations of tested compounds diluted in binding buffer (100 mM HEPES, 0.005% BSA, pH 7.2) to give a total volume of 100 µL per well. After 1 h of incubation, three washes were conducted, and anti-FLAG HRP conjugate was used to detect the bound FLAG-tagged ligand. Plates were washed three times before the addition of 120 µL per well of HRP substrate TMB (3,3′,5,5′-tetramethylbenzidine) and kept in the dark for 15–30 min. The reaction was stopped using 30 µL of 1 M H_2SO_4, and the absorbance value was read at 450 nm. The concentrations of receptors used were 0.3 µg mL^{-1} for CD40, TNFR1 (also known as TNFRSF1A) and RANK (TNFRSF11A); 0.6 µg mL^{-1} for OX40 and 4-1BB (TNFRSF9). The concentrations of the ligands were fixed at 0.02 µg mL^{-1} for CD40L, TNF-α and RANKL; 0.06 µg mL^{-1} for OX40L and 0.1 µg mL^{-1} for 4-1BBL. These values were selected following preliminary testing to optimize response (i.e., to produce a high-enough signal at conditions close to half-maximal response, EC_{50}).

Identification of the binding partner

To determine whether these compounds bind to the receptor OX40 or OX40L, 96-well plates coated with OX40:Fc or OX40L:Fc were first incubated with different concentrations of compounds for 1 h at RT. Then, after three washes with washing solution, the plates were incubated for 1 h with the corresponding tagged ligands (OX40L or OX40 respectively). Plates were then washed three times with washing solution, and the amount of bound partner was detected with secondary antibody anti-tag-peroxidase HRP conjugate followed by reaction with HRP substrate TMB, as described earlier.

Schild analysis

Schild analysis was performed as described previously (Ganesan *et al.*, 2011) using the same set-up described for the PPI binding assay. The plot was constructed by fixing the concentration of OX40 at 0.6 µg mL^{-1}. The concentration of OX40L was varied from 0.001 to 10 µg mL^{-1} by serial dilution to obtain concentration–response curves in the absence or the presence of increasing concentrations (0.4–50.0 µM) of test compound. Binding data were fitted with a unified model as described below in the data fitting subsection.

BrdU incorporation and DAPI exclusion assays

For the BrdU [bromodeoxyuridine (5-bromo-2′-deoxyuridine)] assay, THP-1 human myeloid cells obtained from American Type Culture Collection (ATCC, Manassas, VA, USA) were cultured in RPMI-1640 medium (Invitrogen, Carlsbad, CA, USA) with 10% FBS (v v^{-1}; Invitrogen) and 1% penicillin-streptomycin (v v^{-1}; Invitrogen). THP-1 human myeloid cells were centrifuged and re-suspended in the same medium without FBS and added to a 96-well microtitre plate at a density of 50 000 cells per well in the absence or presence of various concentrations of compounds diluted in the same media. The plate was incubated at 37°C for 24 h. BrdU (5-bromo-2′-deoxyuridine) incorporation level was determined using the BrdU cell proliferation kit from Roche (Mannheim, Germany) according to the manufacturer's protocol. Briefly, BrdU was added to the culture after treatments, and cells were incubated at 37°C for another 6 h. Then, fixing/denaturing buffer was added followed by the addition of HRP-conjugated detection anti-BrdU antibody. BrdU levels were measured using a plate reader at 450 nm after colour development with TMB solution and addition of a stopping solution of H_2SO_4. For the 4′,6-diamidino-2-phenylindol (DAPI) exclusion assay, THP-1 cells were seeded to a density of 500 000 cells mL^{-1} in the absence or presence of test compounds for 24 h. Viability upon treatment was determined using a BD LSR II Flow Cytometer (BD Biosciences, San Jose, CA, USA) and the software FlowJo version 7.2.2 (Ashland, OR, USA). The number of live cells was quantified after gating out DAPI and cell debris assessed on the basis of forward and side-scatter properties of the untreated samples as reference.

Cell transfection

HEK293 cells containing a reporter gene under the control of a minimal promoter fused to NF-κB binding sites (HEK-Blue TNFα/IL-1β cells) were acquired from InvivoGen (San Diego, CA, USA) and further modified to express native or hybrid TNFRSF of interest such as CD40 or OX40. The coding regions of the *CD40* and *OX40* genes were amplified by PCR using as template cDNA of activated CD19$^+$ B cells and activated CD4$^+$ T-cells respectively. Primers were designed from published nucleic acid sequences of CD40 (BC012419) and OX40 (BC105072). Hybrids of receptors OX40 and CD40 were generated via overlapping PCR by fusing the corresponding extracellular regions including signal sequences of OX40 (amino acids 1–214) to a region of the CD40 containing the transmembrane and intracellular domains (amino acids 193–277). After cloning the amplified sequences into the vector pcDNA 3.3-TOPO TA (Invitrogen), the resulting plasmids were transfected into HEK-Blue TNF-α/IL-1β cells. Stable lines resistant to 0.6 mg mL^{-1} of Geneticin (G418; Invitrogen) were analysed by flow cytometry for expression of TNF receptors.

Sensor cell assay

TNFR1, OX40 and CD40 expressing sensor cells were maintained in DMEM at 80% confluence for each experiment. Cells were trypsinized and re-suspended in the same medium with 1% FBS and seeded on 96-well microtiter plates at a density of 100 000 cells per well in the absence and presence of various concentrations of compounds diluted in the same media. For ligand-mediated stimulation, final concentrations of recombinant human TNF-α (20 ng mL^{-1}), CD40L (20 ng mL^{-1}) or OX40L (40 ng mL^{-1}), which have been selected following preliminary testing to optimize response, were maintained in the wells for this purpose. After 18 h of incubation at 37°C, 20 µL of supernatant of each well was taken and added to another 96-well microtitre plate

containing 180 μL per well of QUANTI-Blue (InvivoGen). The level of secreted embryonic alkaline phosphatase (SEAP) was determined after 30 min of incubation at 37°C by reading at 625 nm using a spectrophotometer.

Mice

Foxp3^{GFP} mice were obtained from Dr. A. Y. Rudensky (Memorial Sloan-Kettering Cancer Center, NY, USA) and maintained at the University of Miami. All animal studies were carried out under protocols approved by the University of Miami Institutional Animal Care and Use Committee.

Polarization of naïve CD4⁺ T-cells in vitro

Naïve CD4⁺ T-cells (CD4⁺CD62L⁺Foxp3⁻) obtained from GFP-Foxp3 reporter mice were sorted by flow cytometry, then 100 000 cells per well were activated with anti-CD3 and anti-CD28 conjugated Dynabeads (3 μL per well; Invitrogen). The induction of iT_{reg} cells and T_H9 cells was carried out in the presence of 3 ng mL^{-1} human TGF-β1 (R&D Systems) and 10 ng mL^{-1} IL-2 (PeproTech, Rocky Hill, NJ, USA) for induction of iT_{reg} cells. For T_H9 polarization, 3 ng mL^{-1} human TGF-β1 and 10 ng mL^{-1} IL-4 (PeproTech) were used. In addition, various concentrations of test compound **4** (CVN) diluted in the same media were added along with the Dynabeads and cytokines. CD4⁺ T-cells cultured for 3 days under these polarizing conditions were collected, and cell polarization was assessed by intracellular staining and flow cytometry.

For intracellular cytokine staining, CD4⁺ T-cells activated under T_H9 polarizing conditions were re-stimulated for 4 h with phorbol 12-myristate 13-acetate (50 ng mL^{-1}) and ionomycin (500 ng mL^{-1}; Sigma-Aldrich) in the presence of GolgiStop (BioLegend, San Diego, CA, USA). After being stained with Live/Dead yellow (Sigma-Aldrich), cells were fixed and made permeable with Cytofix/Cytoperm solution (BD Biosciences) and were stained with fluorochrome-conjugated anti-IL-9 (RM9A4; BioLegend). In addition, for the iT_{reg} cell conversion experiment, DAPI staining (Sigma-Aldrich) was used to distinguish live/dead cells, and iT_{reg} cells were identified by the expression of GFP. All samples were acquired with BD LSR II flow cytometer (BD Biosciences), and data were analysed with FACSDiva software (BD Biosciences).

Data fitting and statistics

All binding analyses were carried out in duplicate per plate and repeated at least three times; the averaged data were normalized and used for data fitting and analysis. Binding data were fitted using the standard log inhibitor versus response model in GraphPad Prism (GraphPad, La Jolla, CA, USA):

$$B = 100\frac{[C]}{[C]+IC_{50}} = 100\frac{1}{1+10^{(\log IC_{50}-\log[C])}} \quad (1)$$

For the Schild analysis, a common Gaddum/Schild EC_{50}-shift model was used to fit all binding data obtained at five different inhibitor concentrations:

$$B = B_{bottom} + (B_{top} - B_{bottom})\frac{[L]^{n_H}}{[L]^{n_H} + \left\{K_d\left[1+\left(\frac{[I]}{K_i}\right)^{n_S}\right]\right\}^{n_H}} \quad (2)$$

All fittings were carried out with GraphPad Prism. Cytotoxicity and reporter assay data were analysed by one-way repeated-measures ANOVA followed by Dunnett's multiple comparison *post hoc* test for individual differences using GraphPad Prism and a significance level of $P < 0.05$ for all comparisons.

The NF-κB activation data obtained in the sensor cell assays were fitted with a general quantitative modelling of activation for competitive partial agonists obtained using the minimal 'two-state theory' (del Castillo–Katz) model for receptor activation (Del Castillo and Katz, 1957; Jenkinson, 2003; Bodor and Buchwald, 2012) [mathematically equivalent to the Black and Leff operational model (Black and Leff, 1983; Kenakin, 2006)] when two ligands (L_1, L_2) of different affinities (K_{d1}, K_{d2}) and efficacies (ε_1, ε_2) are present simultaneously. Details of the model are discussed in Supporting Information Appendix S1; the final equation used for fitting was:

$$E = E_{\max}\frac{\varepsilon_1\frac{[L_1]}{K_{d1}} + \varepsilon_2\frac{[L_2]}{K_{d2}}}{1+(1+\varepsilon_1)\frac{[L_1]}{K_{d1}}+(1+\varepsilon_2)\frac{[L_2]}{K_{d2}}} \quad (3)$$

Materials

The monoclonal anti-human OX40L (clone 159403), anti-human CD40L (clone 40804) and anti-human TNF-α antibodies (clone 1825) were purchased from R&D Systems (Minneapolis, MN, USA). Purified recombinant Fc-conjugated receptors (CD40, TNFR1, RANK, OX40, muOX40 and 4-1BB) and their corresponding FLAG-tagged ligands (CD40L, TNF-α, RANKL, OX40L, muOX40L and 4-1BBL) were obtained from Enzo Life Science (San Diego, CA, USA). OX40L:Fc and OX40-His were from Imgenex (San Diego, CA, USA) and Life Technologies (Carlsbad, CA, USA) respectively. Small-molecule compounds of interest are denoted as follows – **1**: DB36 (direct black 36); **2**: DB71 (direct blue 71, CAS 4399-55-7); **3**: DB15 (direct blue 15, CAS 2429-74-5); and **4**: CVN (chlorazol violet N, direct violet 1, CAS 2586-60-9). CVN was from TCI America (Portland, OR, USA); all other chemicals and reagents used were obtained from Sigma-Aldrich (St. Louis, MO, USA).

Results

Effects on the OX40–OX40L binding

Following our recent success in identifying the first small-molecule inhibitors of the CD40-CD40L co-stimulatory interaction within an organic dye-focused library (Margolles-Clark *et al.*, 2009b; 2010; Ganesan *et al.*, 2011), we performed pre-screening assays with this library of several hundred compounds representative of this chemical space for a number of TNFRSF–ligand interactions and identified several compounds (Figure 1) with promising inhibitory activity on the OX40-OX40L binding. Activities were quantified using cell-free *in vitro* assays measuring the amount of soluble human OX40L bound to plate-coated OX40 in the presence of increasing concentrations of test compounds as described previously (Margolles-Clark *et al.*, 2010; Ganesan *et al.*, 2011). Compounds **1**–**4** were selected as some of the most promising

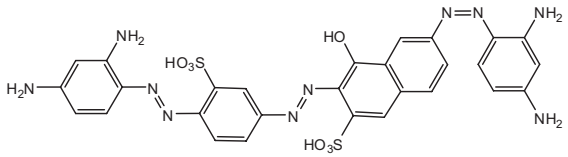

1 (DB36)

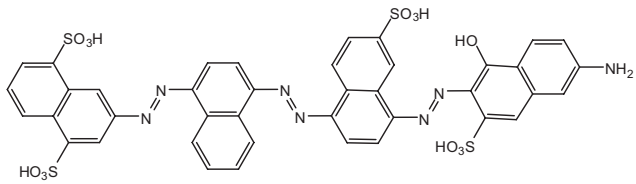

2 (DB71)

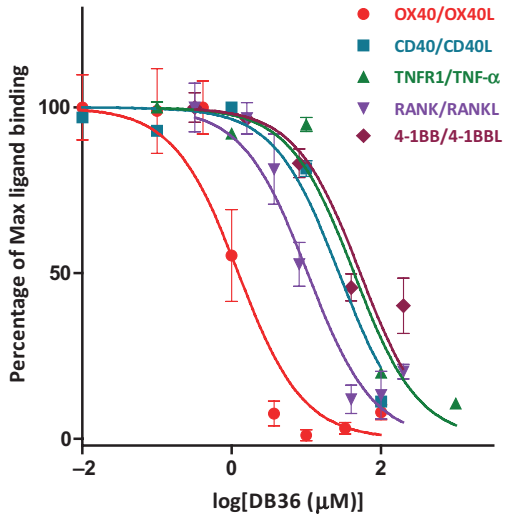

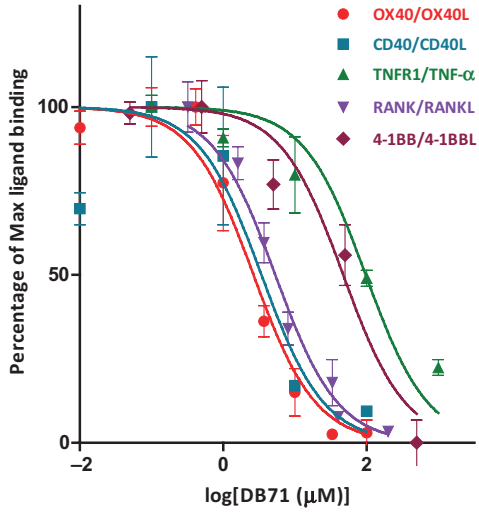

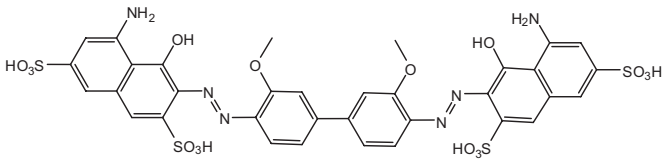

3 (DB15)

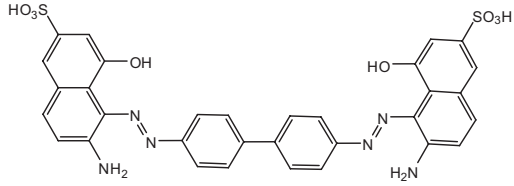

4 (CVN)

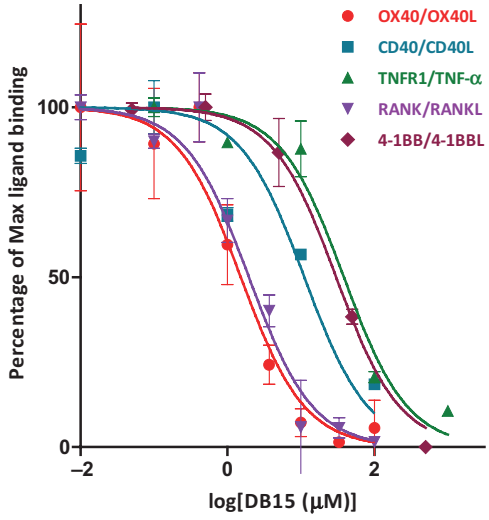

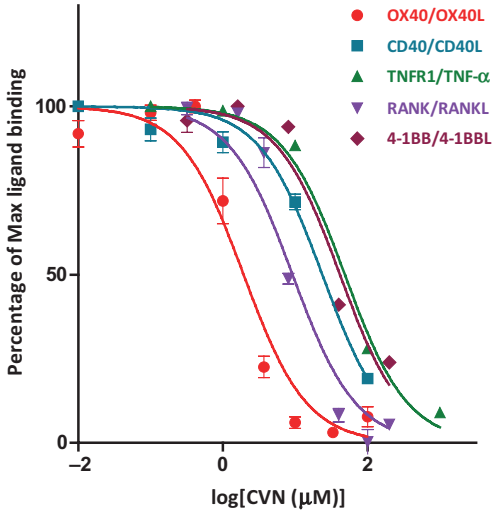

Figure 1

Concentration-dependent inhibition of the OX40–OX40L and other TNFSF ligand–receptor bindings by the small-molecule compounds (**1**–**4**) of the present study with structures as shown (see Table 1 for the corresponding IC_{50}s). Data are average ± SD (normalized to % binding) for $n = 3$ independent experiments with duplicate for each condition.

Table 1

Median inhibitory concentrations (IC_{50}) and their 95% confidence intervals (CI) for compounds **1**–**4** for different TNFRSF-ligand interactions as indicated

	IC_{50} (μM)					
	OX40–OX40L	RANK–RANKL	4-1BB–4-1BBL	CD40–CD40L	TNFR1–TNF-α	OX40 binding*
Compound	Human	Human	Human	Human	Human	Human
1 (DB36)	1.2	10.4	52.9	27.4	43.6	0.4
	[1.0–2.6]	*[8.7–12.6]*	*[39.3–71.1]*	*[21.8–34.4]*	*[33.0–57.5]*	*[0.2–0.7]*
2 (DB71)	2.7	5.3	47.1	3.4	97.3	32.0
	[2.2–3.2]	*[4.7–6.0]*	*[34.4–64.6]*	*[1.9–6.0]*	*[71.6–132.4]*	*[23.7–43.1]*
3 (DB15)	1.5	2.0	30.2	11.1	38.4	2.0
	[1.2–2.0]	*[1.6–2.4]*	*[25.5–35.7]*	*[7.4–16.8]*	*[30.0–49.3]*	*[1.2–3.2]*
4 (CVN)	1.9	9.2	41.4	23.6	48.4	6.6
	[1.5–2.6]	*[7.6–11.1]*	*[33.2–51.6]*	*[19.1–29.3]*	*[42.4–55.3]*	*[4.2–10.5]*
TZ	>2000	>2000	>2000	>2000	>2000	>2000
ErB†	1.7	1.7	10.8	3.1	4.6	1.7
	[1.2–2.6]	*[1.4–2.2]*	*[8.7–13.4]*	*[2.5–3.8]*	*[3.6–5.7]*	*[1.3–2.1]*

Notation for small-molecule compounds – **1**: DB36 (direct black 36); **2**: DB71 (direct blue 71); **3**: DB15 (direct blue 15); **4**: CVN (chlorazol violet N, direct violet 1.
*IC_{50} values obtained in the binding partner assay. CI shown in italic font and in square parentheses.
†Values obtained in Ganesan *et al.* (2011), except for the last column, which was measured here.
TZ, tartrazine; ErB, erythrosine B.

ones that concentration-dependently inhibited the OX40-OX40L binding with low micromolar potency (Figure 1). As before, tartrazine was included as a negative control in all assays since it is a polysulfonated dye with a chemical structure somewhat related to those of **1**–**4** that, however, consistently showed no activity in any of these assays. Median inhibitory concentrations (IC_{50}s) obtained by fitting the data with a standard binding model were 1.2, 2.7, 1.5 and 1.9 μM for **1**, **2**, **3** and **4**, respectively, and are summarized in Table 1. All binding assays were performed at room temperature (25°C), but for verification purposes, we have also performed them at body temperature (37°C) for compounds **1**–**4** and observed no significant differences (i.e., no IC_{50} changed by more than 35%, within the experimental error; data not shown). As before for the CD40-CD40L system (Margolles-Clark *et al.*, 2009b), in addition to the human proteins, the binding assay was also performed with mouse OX40 and OX40L. Whereas the human antibody inhibited only the human system, the small molecules showed similar inhibitory activity in both systems (data not shown).

Specificity (within TNFSF) and cytotoxicity

Besides activity, selectivity towards the desired target also has to be defined. Accordingly, for compounds of interest, in addition to OX40-OX40L, we quantified inhibitory activities towards several other ligand–receptor pairs within the TNF superfamily, such as TNFR1-TNFα, CD40-CD40L, RANK-RANKL and 4-1BB-4-1BBL. While **1** and **4** showed acceptable (>5–20-fold) selectivity towards OX40–OX40L interaction when compared to all other TNFSF interactions tested, **2** and **3** showed similar activity toward CD40-CD40L and RANK-RANKL, respectively, as they inhibited these interactions with IC_{50}s comparable to that for OX40-OX40L (Figure 1; Table 1). For comparison, data for erythrosine B, a promiscuous PPI inhibitor we have identified earlier that shows no specificity and inhibits a variety of interaction with IC_{50}s consistently in the 2–20 μM range (Ganesan *et al.*, 2011), were also included in Table 1.

For the most promising compounds, we also performed brief cytotoxicity evaluations in THP-1 (human monocytic leukaemia) cells. Toxic effects were assessed by a standard cell proliferation assay (BrdU incorporation) as well as a viability assay (DAPI exclusion). In the BrdU assay, none of the compounds showed cytotoxicity with IC_{50}s less than 100 μM (well above the range of OX40-OX40L inhibitory activities); however, **2** inhibited cell proliferation at the highest concentration of 500 μM (Supporting Information Figure S1). Interestingly, some compounds such as **1** and **3** increased BrdU incorporation indicating a possibly increased proliferation rate. Toxic effects were also assessed by an additional viability assay (DAPI exclusion analysed by flow cytometry), and results confirmed well the observations of the BrdU assay with only **2** showing some cytotoxicity at the higher concentrations (Supporting Information Figure S2).

Binding partner and nature of OX40-OX40L binding inhibition

To elucidate the mechanism of the observed binding inhibition, we first performed experiments to assess whether these compounds bind to the receptor (OX40) or its ligand partner (OX40L). Similar experiments with our previously identified CD40-CD40L PPIIs showed that the most active compounds in that assay bind to the surface of CD40L, but not CD40 (Margolles-Clark *et al.*, 2009b). Plate-coated proteins (OX40:Fc or OX40L:Fc, respectively) were incubated for 1 h with increasing concentrations of the test compounds, and after three washes to eliminate the unbound small molecules, the abilities to still bind the corresponding protein partner (OX40L or OX40, respectively) were assessed. Since our compounds bound with low micromolar affinities, we conducted preliminary assessments of the binding kinetics, which indicated that the binding was sufficiently long-lasting to make this assay feasible (data not shown). Results (Figure 2) indicate OX40 as the binding site for all of these compounds as they showed inhibition with IC_{50}s in general agreement with those obtained for their previous interaction inhibitory activity (Figure 1; Table 1). None of the compounds tested bound OX40L, except for the promiscuous PPI inhibitor erythrosine B (Ganesan *et al.*, 2011).

As a further mechanistic evaluation, we performed a Schild analysis (Kenakin, 2006; Ganesan *et al.*, 2011) with **4** as our most promising representative compound to assess the competitive/reversible nature of this binding. Concentration-dependency curves were generated by using a fixed concentration of OX40 and varying concentrations of OX40L in the presence of increasing concentrations of **4**. Data from this complex binding assay (Supporting Information Figure S3) could be fitted well with the unified Gaddum–Schild model (Eq. 2), indicating that **4** interferes with the OX40-OX40L binding in a manner that is consistent with a competitive binding interaction. The fit indicated a K_d of approximately 5 nM for the binding of the protein receptor–ligand pair (OX40-OX40L) and a pK_B value of 5.9 (corresponding to K_B of 1.2 μM; 95% CI: 0.6–2.4 μM) for the binding of **4**, in good agreement with data obtained in the plain binding experiment (1.9 μM, Table 1).

Effect in sensor cells with NF-κB reporter

To confirm the activity of the identified most promising compounds in a cell-based model, we used sensor cells containing a SEAP reporter gene under the control of a promoter fused to NF-κB binding site and transfected them with several receptors within the TNFRSF, including OX40, as described in the Methods section. Thus, in these cells the secretion of SEAP is specifically induced by the binding of a particular TNFSF ligand to its corresponding cell-surface receptor that all have a shared downstream activation of the NF-κB pathway. We confirmed that the OX40-transfected cells are indeed activated by OX40L in a concentration-dependent manner (Supporting Information Figure S4). Intriguingly enough, for compounds **1**–**4**, which all inhibited OX40-OX40L binding in the cell-free binding assay, we could not see inhibition. Rather, they all showed a concentration-dependent enhancement of the OX40-linked activation of NF-κB in these sensor cells in the presence of a fixed concentration (100 ng mL^{-1} ≈

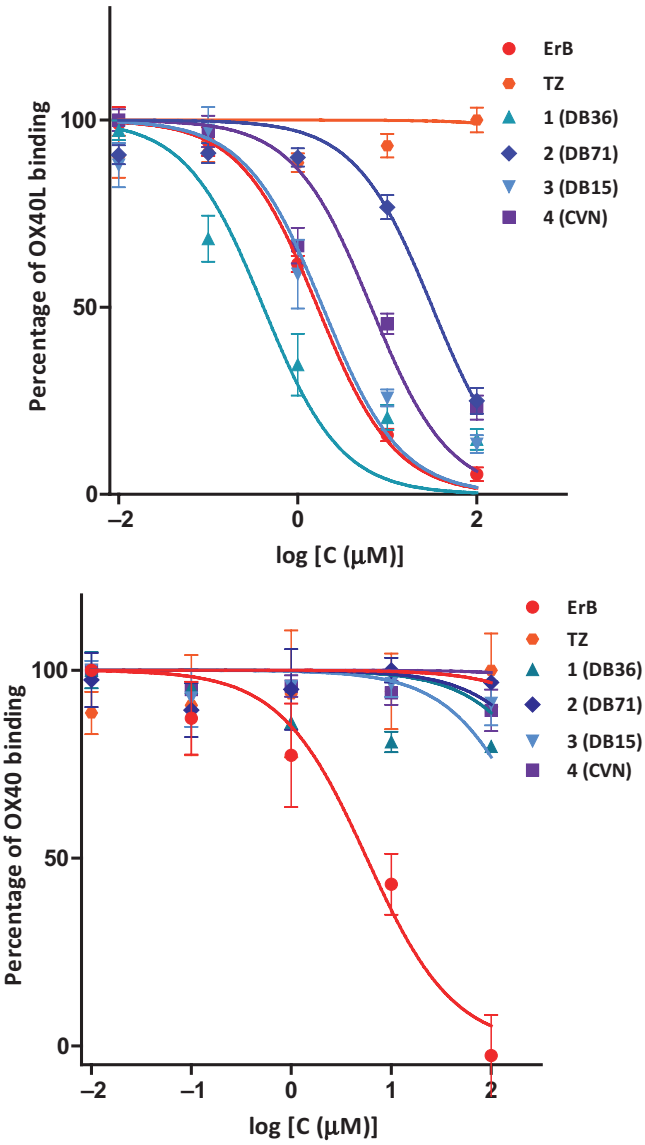

Figure 2

Identification of the binding partner (OX40 or OX40L) by assessing the amount of OX40L (top) or OX40 receptors (bottom) bound after incubations of the candidate compounds with OX40 receptors or OX40L, respectively, and addition of the protein binding partner (OX40L or OX40) only after a wash-out. All tested compounds bind to OX40 receptors, while only the promiscuous PPI inhibitor erythrosine B (ErB) binds to OX40L. Data are average ± SD (normalized to percent binding) for n = 3 independent experiments with triplicate for each condition.

3.3 nM) of recombinant OX40L with **1** and **4** showing the most potency (Supporting Information Figure S3). This, in combination with the previous results, suggested the possibility that these tested compounds cannot only compete for binding to OX40 with its innate OX40 ligand, but might also have the potential to activate the OX40 signalling downstream. To test whether the presence of OX40 ligand is required for the stimulation of OX40 signalling by the small-molecule compounds, we incubated the sensor cells with

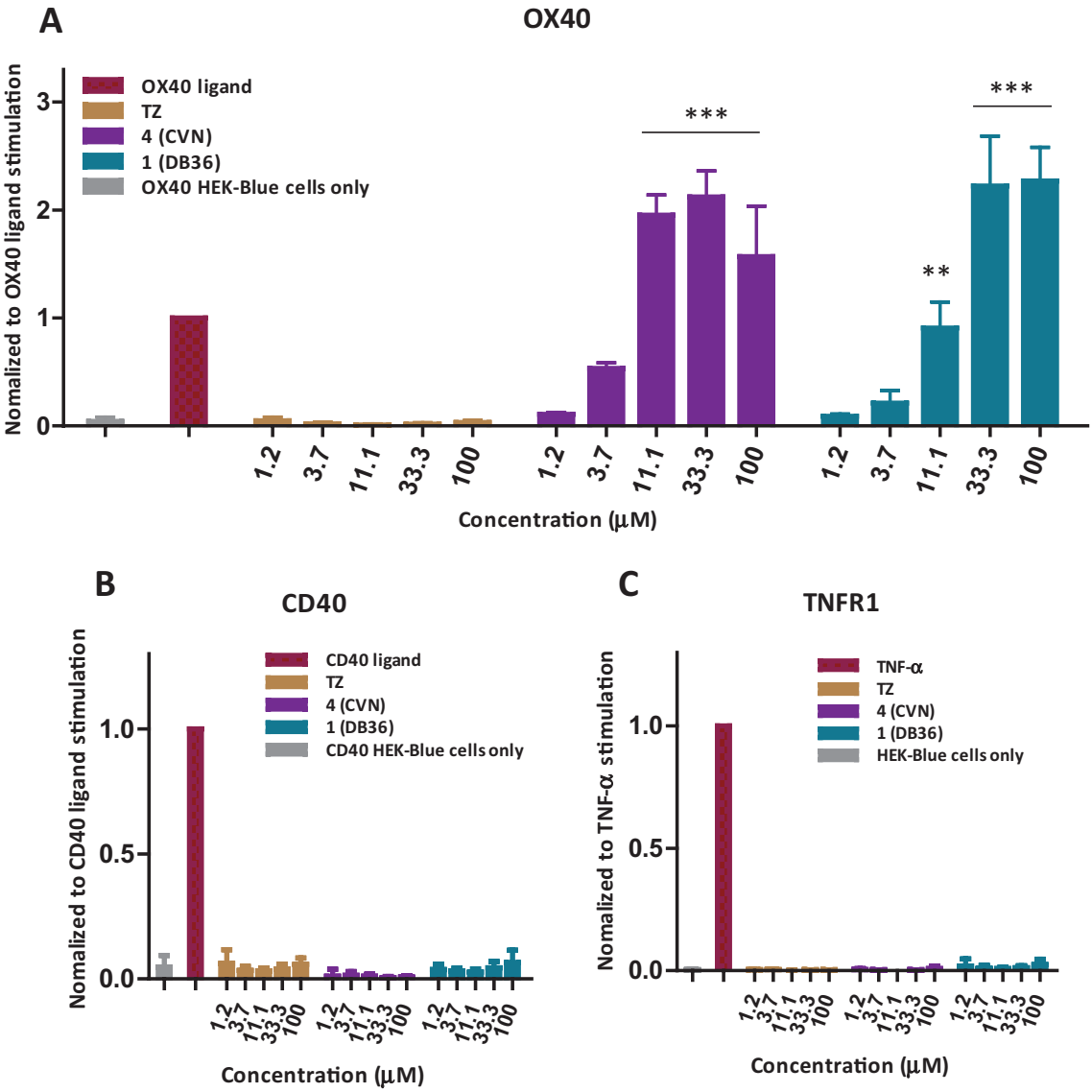

Figure 3

Selective stimulatory activity of **1** (DB36) and **4** (CVN) in OX40-transfected NF-κB sensor cells (A) as compared to total lack of such effect in similar CD40 (B) and TNFR1 (C) sensor cells. Data (average ± SD for $n = 3$ independent experiments with triplicate for each condition) were analysed by ANOVA with Dunnett's multiple comparison *post hoc* test. $^{**}P < 0.01$ and $^{***}P < 0.001$ as compared with control (cells incubated without any stimulation).

increasing concentrations of **1** and **4** and quantified NF-κB activation via SEAP. Interestingly, both compounds clearly increased SEAP secretion in concentration-dependent manner even without the presence of recombinant OX40L; however, they could not produce the same maximum activation. Furthermore, the activation by **1** and **4** was target specific as they did not activate the downstream NF-κB pathway when incubated with either TNFR1 or CD40 expressing sensor cells (Figure 3).

As a next step, to clarify the agonistic nature of these compounds, we quantified in detail the concentration dependence of the NF-κB activation caused in these sensor cells by combinations of **4** and the natural ligand OX40L at various concentrations. In the absence of OX40L (or in the presence of low concentrations of OX40L), **4** was able to produce concentration-dependent increase in NF-κB activation, but with a maximum that even at saturation was only a fraction of that produced by the natural ligand OX40L (Figure 4). In the presence of sufficiently high OX40L (1000 ng $mL^{-1} \approx 33$ nM), **4** actually produced a slight decrease of activation in a concentration-dependent manner (Figure 4), a behaviour typical for partial agonists (Jenkinson, 2003; Kenakin, 2006). To verify this, we performed a quantitative modelling of the activation using a generalization of the minimal 'two-state theory' (del Castillo–Katz) model for receptor activation (Del Castillo and Katz, 1957; Jenkinson, 2003; Bodor and Buchwald, 2012) [mathematically equivalent with the Black and Leff operational model (Black and

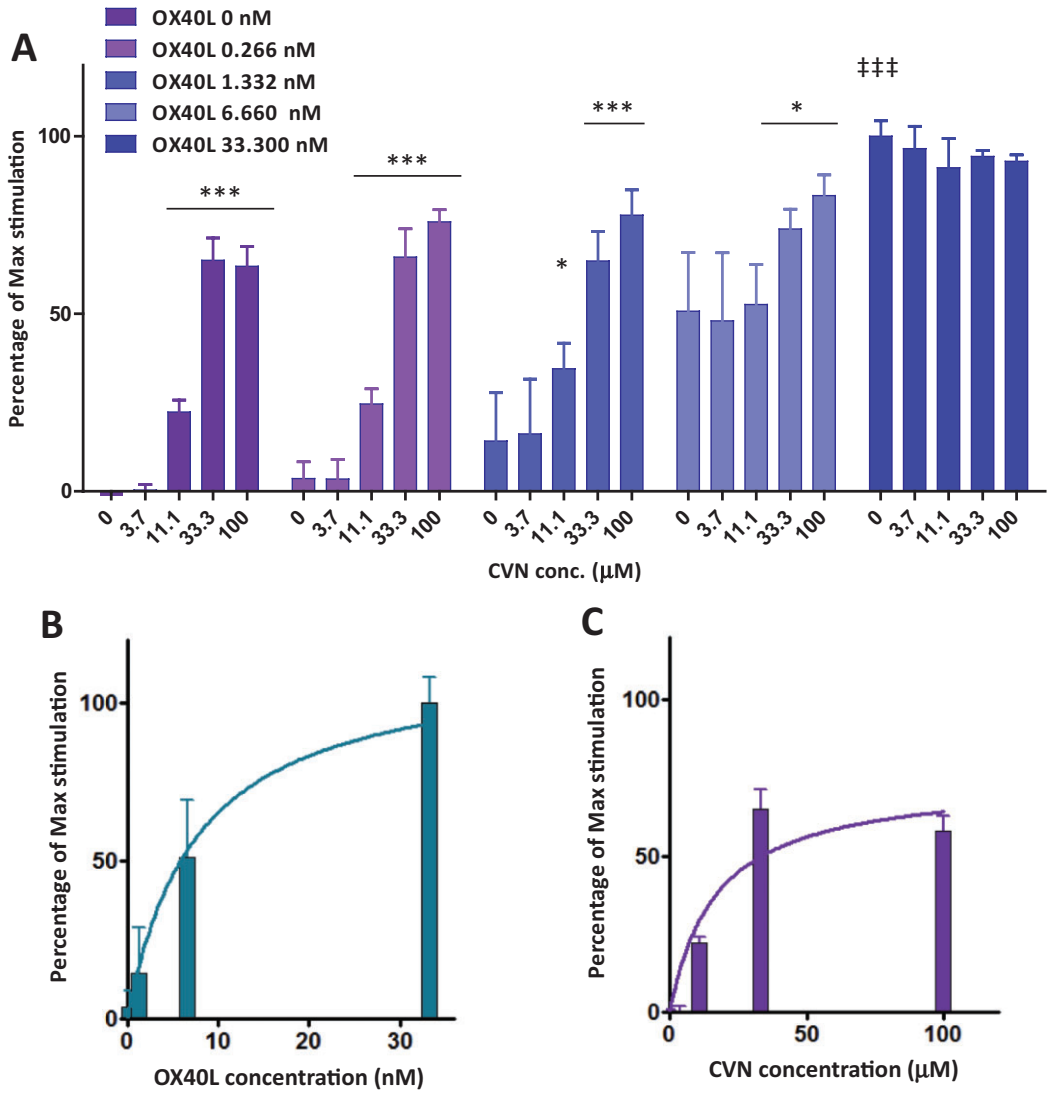

Figure 4

Activation of OX40 NF-κB reporter cells by OX40L and **4** combined at various concentrations. (A) OX40 sensor cells with NF-κB-induced SEAP were incubated overnight with a combination of both serial diluted OX40L and **4**. Results are represented as the absorbance value of collected cell supernatant at the wavelength of 650 nm. Asterisks denote statistically significant differences compared to CVN 0 within each OX40L group (*$P < 0.05$, ***$P < 0.001$); double daggers denote ‡‡‡$P < 0.001$ between the maxima of OX40L alone (OX40L 33.3 nM, CVN 0) versus CVN alone (OX40L 0, CVN 100 μM) (ANOVA with Dunnett's multiple comparison *post hoc* test). As compared to OX40L (B), **4** (CVN) alone (C) only achieved a maximum activation of the OX40-triggered response that was about 70%, indicating a partial agonist type response in this system.

Leff, 1983; Kenakin, 2006)] for the case of two ligands (L_1, L_2) of different affinities (K_{d1}, K_{d2}) and efficacies (ε_1, ε_2) simultaneously present (eq. 3, see Supporting Information Appendix S1 for full details). Fitting of the model to the data (Figure 5) shows that assumptions of a partial agonist with an efficacy of about 70% of that of OX40L can indeed account well for the behaviour seen, including the concentration-dependent decrease of activation produced in the presence of the highest concentration of the natural ligand OX40L. The affinity (K_d) values derived from this cell-based assay, as fitted with a unified model, are somewhat lower but still in acceptable agreement with those obtained in previous cell-free assays (approximately 11 nM for OX40L and 17 μM for **4** obtained by fitting an equation equivalent to eq. 3, but with efficacies incorporated into different E_{max}s).

Effect on T-cells (T_{reg} and T_H9)

Regulatory T-cells (T_{regs}) are known to play important immunomodulatory roles, and OX40 agonist signalling has been shown to suppress the generation of induced regulatory T-cells (iT_{regs}) (So and Croft, 2007; Xiao *et al.*, 2012). To validate the stimulatory activity on OX40 signalling of our small-molecule partial agonists, we performed iT_{reg} conversion experiments using flow cytometry sorted naïve $CD4^+$ T_{conv} cells ($CD62L^+$ $Foxp3^-$) from *Foxp3*-GFP reporter mice with our most promising representative compound (**4**, CVN). They

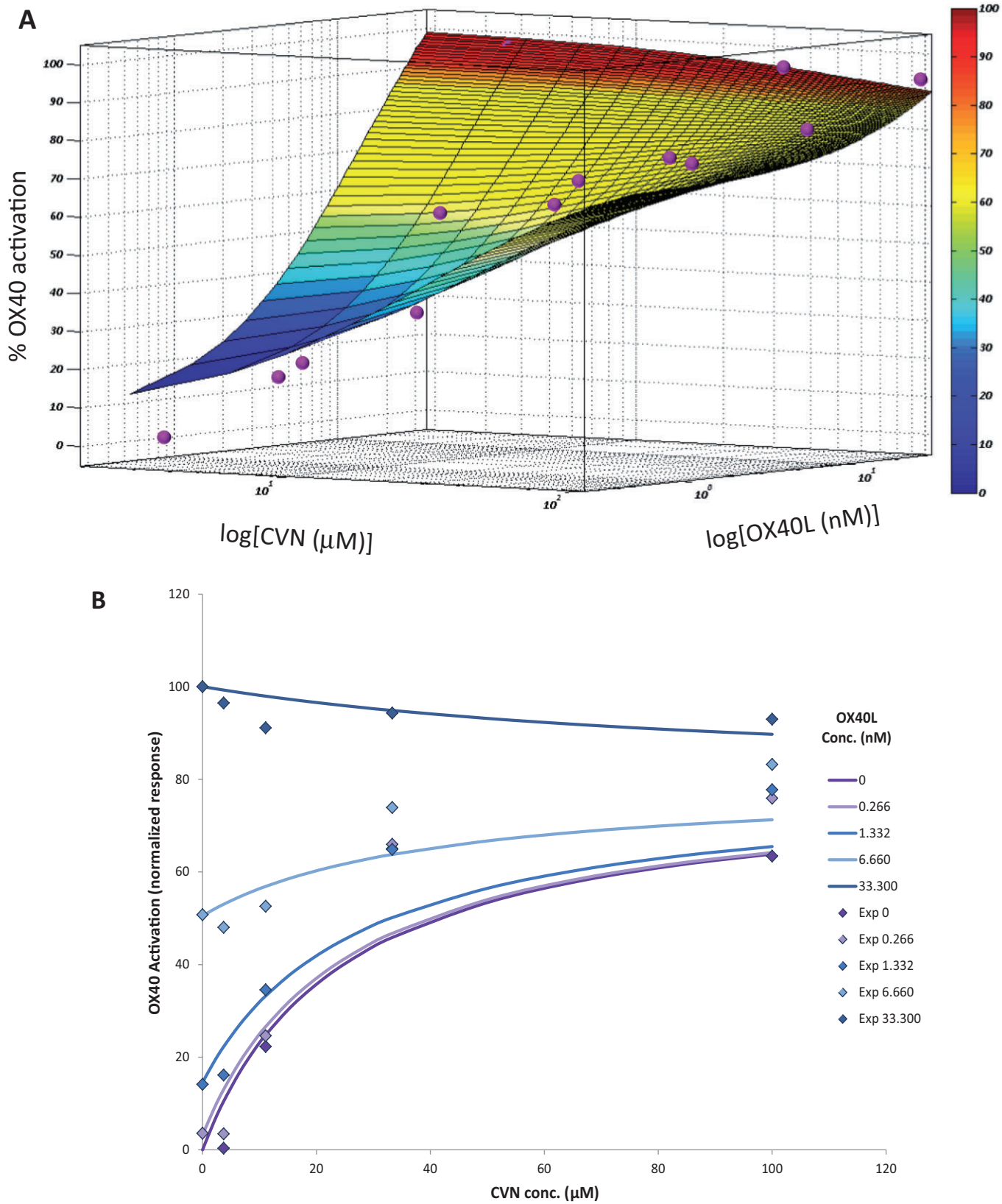

Figure 5

Three-dimensional surface representation of the activation effect on OX40 by a combination of full agonist OX40L and partial agonist **4** (CVN) in sensor cells with an NF-κB reporter (A). Purple dots represent experimental data and the surface calculated values by the corresponding fitted model (Eq. 3). Concentrations are on the horizontal axes and are on log scales. The bottom figure (B) shows a corresponding two-dimensional representation (essentially equivalent with a cross-sectional view of the top figure from left, front) with a linear concentration scale.

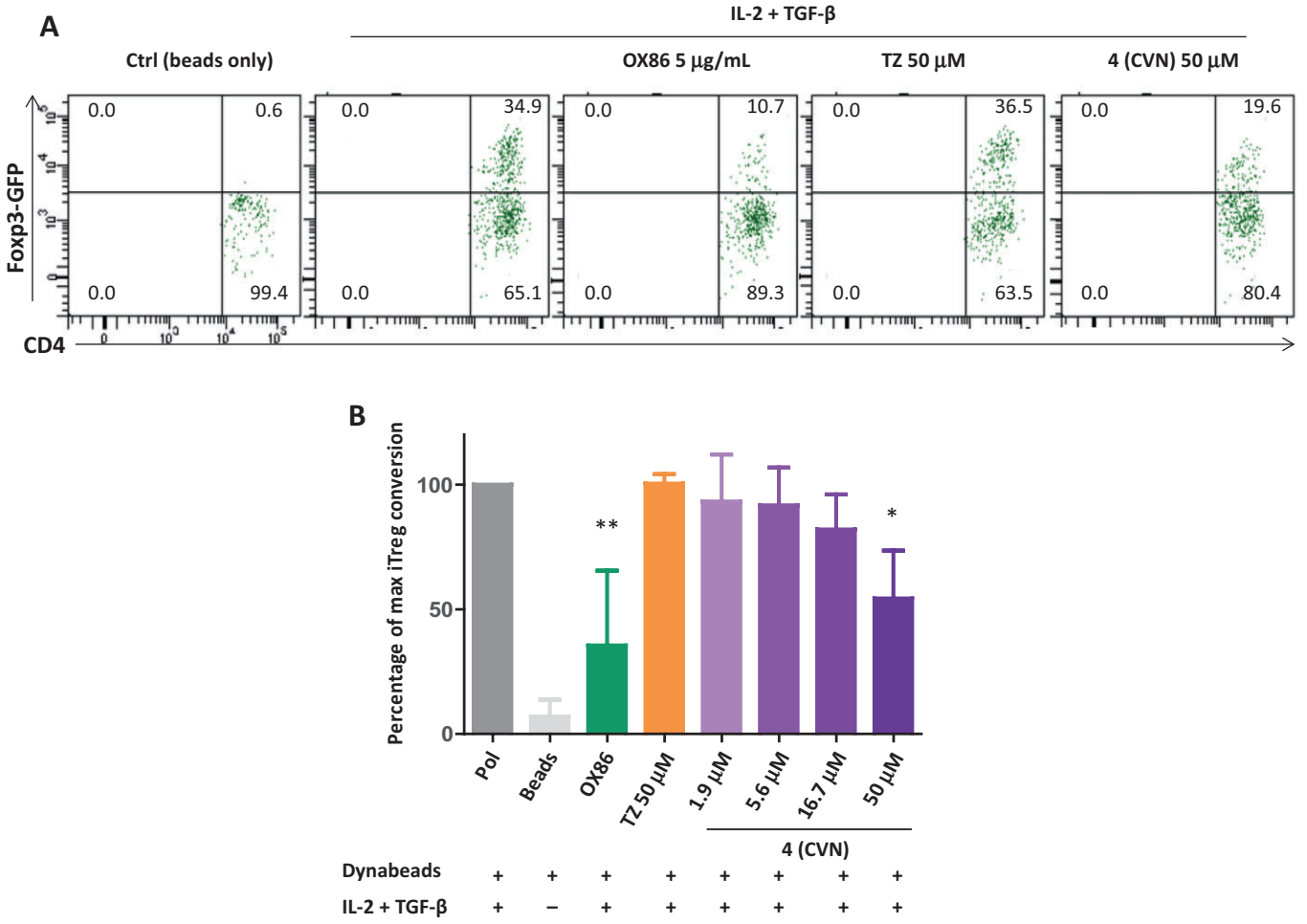

Figure 6

Compound **4** inhibits iT_{reg} generation. (A) Naïve wild-type $CD4^+$ T-cells were activated for three days (Dynabeads plus iT_{reg} polarizing cytokines, IL-2 + TGF-β) by increasing concentrations of **4** (CVN). Agonist OX40 antibody (OX86) and tartrazine (TZ) were added as positive and negative controls respectively. Inhibitory effect on the induction of iT_{reg} cells were accessed by gating on the live $CD4^+$ T-cell population. (B) Summary of all experiments showing average ± SD of three independent replicates. Data were analysed by ANOVA with Dunnett's *post hoc* test with $*P < 0.05$ and $**P < 0.01$ as compared with T_{reg} polarizing conditions (IL-2 + TGF-β).

were activated *in vitro* under iT_{reg} polarizing conditions (TGF-β plus IL-2) and then assessed for Foxp3 induction. After 3 days of incubation, approximately 30% of $CD4^+$ T_{conv} cells were converted into $Foxp3^+$ iT_{reg} cells in the presence of anti-CD3 and anti-CD28 magnetic beads (Dynabeads) plus TGF-β and IL-2. The agonistic anti-OX40 monoclonal antibody (mAb) (OX86) used as a positive control indeed inhibited iT_{reg} conversion, and small-molecule **4**, a partial agonist, also showed a less potent, but concentration-dependent inhibition with significant inhibition at 50 µM (Figure 6).

Stimulation on OX40 has also been shown to enhance T_H9 cell generation in *vitro* (Xiao *et al.*, 2012). Therefore, as a further test of the OX40 partial agonist nature, we incubated **4** with naive $CD4^+$ T_{conv} cells in the presence of anti-CD3 and anti-CD28 conjugated beads plus T_H9 cell polarization conditions (TGF-β plus IL-4) for 3 days, re-stimulated with PMA/ionomycin for 4 h in the presence of Golgi stop, and assessed IL-9 levels by intracellular staining. The OX40 agonistic antibody (OX86) significantly enhanced T_H9 cell percentage (by approximately 35%; Figure 7). Compound **4** also caused less prominent, but statistically significant enhancement of the T_H9 cell population: approximately 15% at 50 µM versus approximately 5% of control (TGF-β plus IL-4 only) (Figure 7).

Discussion

As part of our ongoing search for potential therapeutically useful small-molecule modulators of co-stimulatory signalling, we have now identified the first small-molecule compounds capable of interfering with the OX40-OX40L PPI that also seem to act as partial agonists at the OX40 receptor. This is remarkable not only because PPIs have been traditionally considered untreatable with small-molecule inhibitors [with some success achieved only within the last decade or so (Arkin and Wells, 2004; Whitty and Kumaravel, 2006; Wells and McClendon, 2007; Buchwald, 2010)], but also because

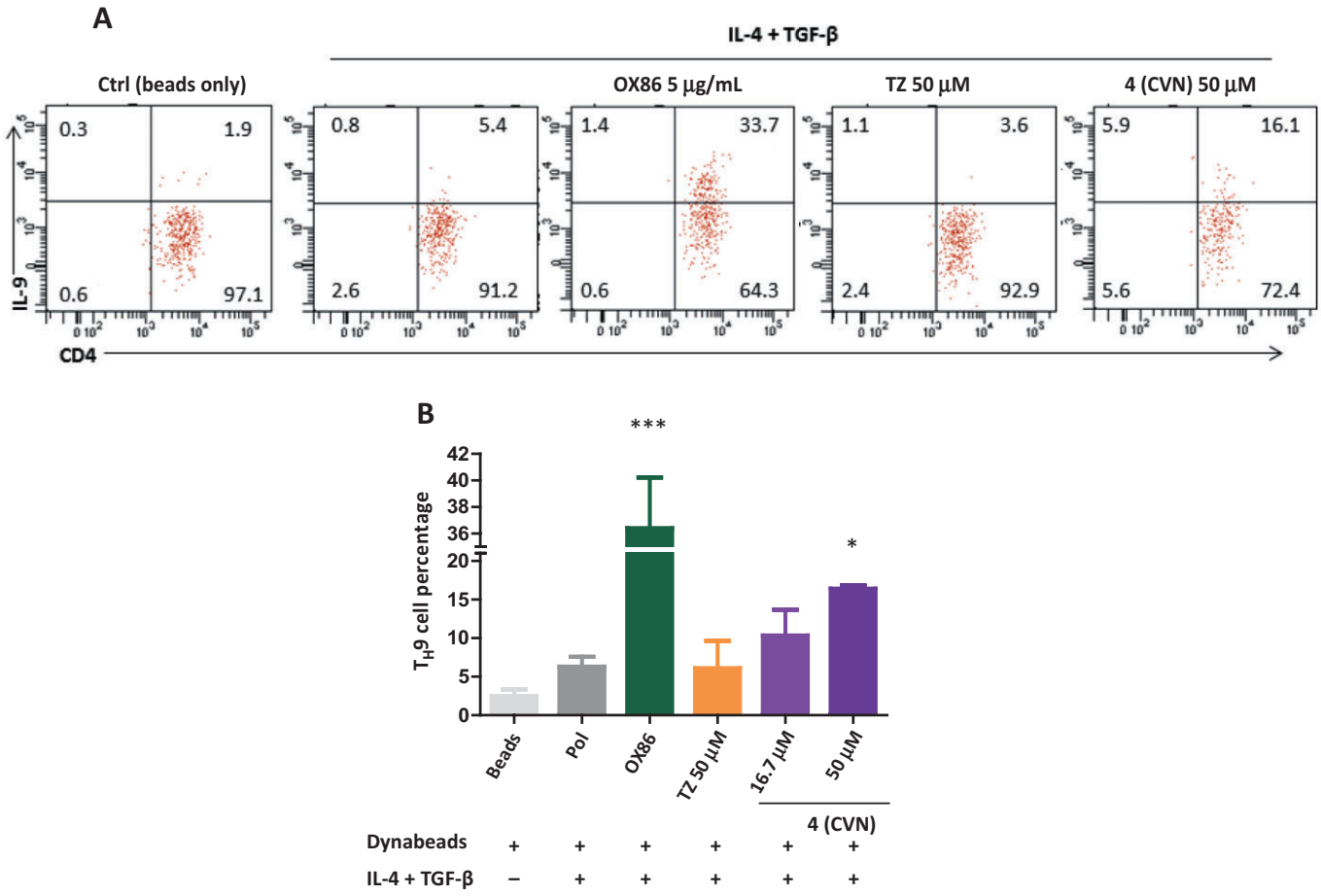

Figure 7

Compound **4** enhances the induction of T_H9 cells. (A) Naïve wild-type $CD4^+$ T-cells were activated for three days (Dynabeads plus iT_{reg} polarizing cytokines, IL-4 + TGF-β) by increasing concentrations of **4** (CVN). Agonist OX40 antibody (OX86) and tartrazine (TZ) were added as positive and negative controls, respectively. Stimulatory effects on the induction of T_H9 cells were accessed by gating on the live $CD4^+$ T-cell population. (B) Summary of all experiments showing average ± SD. Data were analysed by ANOVA with Dunnett's *post hoc* test with $^*P < 0.05$ and $^{***}P < 0.001$ as compared with T_H9 polarizing conditions (IL-4 + TGF-β).

small-molecule PPI agonists are considered even less likely to exist since, in addition to binding, they also need to be able to trigger the downstream activation. Not surprisingly, only a very limited number of small-molecule PPI 'agonists' (i.e., enhancers or stabilizers) have been published to date (Rose *et al.*, 2010; Milroy *et al.*, 2013; Ottmann, 2013; Wang *et al.*, 2013). The TNFRSF family has many high-value therapeutic targets, and biological compounds targeting almost all of the more than twenty known ligand–receptor pairs in this superfamily are now in clinical development for autoimmune diseases and cancer respectively (Tansey and Szymkowski, 2009; Croft *et al.*, 2013; Yao *et al.*, 2013). In the meantime, only very few small-molecule PPI inhibitors have been identified for TNFSF; they include one for TNFR1-TNF-α (SP307) (He *et al.*, 2005) as well as some polyaromatic inhibitors for the CD40-CD40L co-stimulatory interaction including those by our group (Margolles-Clark *et al.*, 2009b; 2010) and another, quite different scaffold (BIO8898) from Biogen (Silvian *et al.*, 2011). SP307 was found to bind the TNF-α trimer and facilitate its dissociation (He *et al.*, 2005), whereas BIO8898 was found to bind between two subunits of the CD40L trimer and distort it sufficiently to disrupt its binding with CD40 (Silvian *et al.*, 2011).

By starting from the chemical space of organic dyes that provided our first CD40-CD40L PPIIs, we have now identified what seem to be the first small-molecule disruptors of the OX40-OX40L PPI that also act as partial agonists of the OX40 receptor with low micromolar potency. Detailed quantitative data support its partial agonist nature indicating that it causes agonism when no other agonists are present, but antagonism of more powerful (full) agonists (here, OX40L) if they are present. The activity of **4** (CVN, Figure 1) has been confirmed in sensor cell assays (Figure 4) as well as in T-cells, including T_{reg} and T_H9 cells (Figure 6, Figure 7). Compared with the binding assay, activities in the cell-based assays are lower – probably, partly due to nonspecific protein binding in the presence of protein-rich media, as observed previously with similar compounds by us (Margolles-Clark *et al.*, 2009b; 2010), and partly due to the interactions with other cell-surface TNFRSF and other receptors confounding the effect

especially as the OX40 receptor is only transiently expressed in T-cells. OX40 (CD134), a member of the TNFRSF superfamily, is mainly expressed on activated T-cells. Conflicting data regarding the role of OX40 agonists on the persistence and function of regulatory T-cells (T_{regs}) have revealed that OX40 signalling plays a complex role in the physiology of T_{regs} (Takeda *et al.*, 2004; Valzasina *et al.*, 2005; Ito *et al.*, 2006; Kroemer *et al.*, 2007; So and Croft, 2007; Vu *et al.*, 2007; Duan *et al.*, 2008; Piconese *et al.*, 2008; Redmond *et al.*, 2009; Ruby *et al.*, 2009; Griseri *et al.*, 2010; Kinnear *et al.*, 2013). Nevertheless, there is compelling evidence supporting a suppressive effect of OX40 agonism on the development of T_{regs} *in vitro*. In addition, under an appropriate cytokine microenvironment (in the presence of TGF-β and IL-4), OX40 stimulation has been demonstrated to induce T_H9 cell generation (Xiao *et al.*, 2012). Consistent with these findings, our small-molecule OX40 partial agonist **4** showed less prominent, but similar activity to that of the OX40 agonistic mAb (OX86) when tested in these models relying upon the induction of T_{reg} and T_H9 cells from naive $CD4^+$ T-cells.

Preclinical data from tumour models and clinical data from breast cancer patients have suggested the beneficial effect of OX40 agonists (either OX40L:Ig fusion protein or OX40 agonist antibody) on tumour progression (Weinberg *et al.*, 2011). Both $CD4^+$ and $CD8^+$ T-cells seem to be involved in the therapeutic efficacy of OX40 agonists. Due to the inducible and time-limited expression of OX40 on these cells, therapies targeting OX40 might produce less toxicity and reduced systemic side effects than existing immunomodulatory therapies in clinical use. Consequently, several biological candidates targeting this pathway are in various stages of clinical development (Tansey and Szymkowski, 2009; Croft *et al.*, 2013; Sheridan, 2013; Yao *et al.*, 2013). Furthermore, and of particular interest for our autoimmune disease-focused work, recently it has been shown that OX40 stimulation can promote T_{reg} expansion *in vivo* in both mouse models of diabetes and colitis, which, in turn, prevented diabetes onset and suppressed colitis (Griseri *et al.*, 2010; Bresson *et al.*, 2011). The dual function of OX40 agonists to increase T-cell effector function as well as regulate T_{reg} function selectively in different pathological conditions renders OX40 agonism a promising therapeutic possibility for the prevention of these diseases. Our proof-of-principle results identifying the first small molecules that can act as disruptors of the OX40-OX40L PPI as well as partial OX40 agonists represent a first step towards identifying new pharmacological tools to investigate this interaction that could also lead to possible therapeutic alternatives complementing the current biological drugs under development.

Acknowledgement

This work was supported by a grant from the National Institutes of Health National Institute of Allergy and Infectious Diseases (1R01AI101041-02, PI: P. B.).

Author contributions

Y. S. performed the experiments, collected data, analysed results and wrote the manuscript. E. M.-C. prepared the transfected lines and performed experiment. A. B. and Y. S. designed the mouse immunology experiments and analysed the results. P. B. conceived the study, designed the experiments, analysed data and results, and wrote the manuscript. All authors reviewed the final manuscript.

Conflict of interest

The authors declare that they have no competing financial interest.

References

Alexander SPH, Benson HE, Faccenda E, Pawson AJ, Sharman JL, Spedding M *et al.* (2013). The Concise Guide to PHARMACOLOGY 2013/14: Catalytic receptors. Br J Pharmacol 170: 1676–1703.

Arkin MR, Wells JA (2004). Small-molecule inhibitors of protein-protein interactions: progressing towards the dream. Nat Rev Drug Discov 3: 301–317.

Black JW, Leff J (1983). Operational models of pharmacological agonism. Proc R Soc Lond B Biol Sci 220: 141–162.

Bodor N, Buchwald P (2012) Retrometabolic Drug Design and Targeting, 1st edn. Wiley: Hoboken, NJ.

Bresson D, Fousteri G, Manenkova Y, Croft M, von Herrath M (2011). Antigen-specific prevention of type 1 diabetes in NOD mice is ameliorated by OX40 agonist treatment. J Autoimmun 37: 342–351.

Buchwald P (2010). Small-molecule protein-protein interaction inhibitors: therapeutic potential in light of molecular size, chemical space, and ligand binding efficiency considerations. IUBMB Life 62: 724–731.

Chen M, Xiao X, Demirci G, Li XC (2008). OX40 controls islet allograft tolerance in CD154 deficient mice by regulating $FOXP3^+$ Tregs. Transplantation 85: 1659–1662.

Cheng AC, Coleman RG, Smyth KT, Cao Q, Soulard P, Caffrey DR *et al.* (2007). Structure-based maximal affinity model predicts small-molecule druggability. Nat Biotechnol 25: 71–75.

Cochran AG (2000). Antagonists of protein-protein interactions. Chem Biol 7: R85–R94.

Croft M (2010). Control of immunity by the TNFR-related molecule OX40 (CD134). Annu Rev Immunol 28: 57–78.

Croft M, So T, Duan W, Soroosh P (2009). The significance of OX40 and OX40L to T-cell biology and immune disease. Immunol Rev 229: 173–191.

Croft M, Benedict CA, Ware CF (2013). Clinical targeting of the TNF and TNFR superfamilies. Nat Rev Drug Discov 12: 147–168.

Del Castillo J, Katz B (1957). Interaction at end-plate receptors between different choline derivatives. Proc R Soc Lond B Biol Sci 146: 369–381.

Dollins CM, Nair S, Boczkowski D, Lee J, Layzer JM, Gilboa E *et al.* (2008). Assembling OX40 aptamers on a molecular scaffold to create a receptor-activating aptamer. Chem Biol 15: 675–682.

Duan W, So T, Croft M (2008). Antagonism of airway tolerance by endotoxin/lipopolysaccharide through promoting OX40L and suppressing antigen-specific $Foxp3^+$ T regulatory cells. J Immunol 181: 8650–8659.

Ganesan L, Margolles-Clark E, Song Y, Buchwald P (2011). The food colorant erythrosine is a promiscuous protein-protein interaction inhibitor. Biochem Pharmacol 81: 810–818.

Griseri T, Asquith M, Thompson C, Powrie F (2010). OX40 is required for regulatory T cell-mediated control of colitis. J Exp Med 207: 699–709.

He MM, Smith AS, Oslob JD, Flanagan WM, Braisted AC, Whitty A *et al.* (2005). Small-molecule inhibition of TNF-α. Science 310: 1022–1025.

Hopkins AL, Groom CR (2002). The druggable genome. Nat Rev Drug Discov 1: 727–730.

Ishii N, Takahashi T, Soroosh P, Sugamura K (2010). OX40-OX40 ligand interaction in T-cell-mediated immunity and immunopathology. Adv Immunol 105: 63–98.

Ito T, Wang YH, Duramad O, Hanabuchi S, Perng OA, Gilliet M *et al.* (2006). OX40 ligand shuts down IL-10-producing regulatory T cells. Proc Natl Acad Sci USA 103: 13138–13143.

Jenkinson DH (2003). Classical approaches to the study of drug-receptor interactions. In: Foreman JC, Johansen T (eds). Textbook of Receptor Pharmacology, 2nd edn. CRC Press: Boca Raton, FL, pp. 3–80.

Kenakin TP (2006). A Pharmacology Primer: Theory, Applications, and Methods, 2nd edn. Academic Press: San Diego, CA.

Kinnear G, Wood KJ, Fallah-Arani F, Jones ND (2013). A diametric role for OX40 in the response of effector/memory $CD4^+$ T cells and regulatory T cells to alloantigen. J Immunol 191: 1465–1475.

Kjaergaard J, Tanaka J, Kim JA, Rothchild K, Weinberg A, Shu S (2000). Therapeutic efficacy of OX-40 receptor antibody depends on tumor immunogenicity and anatomic site of tumor growth. Cancer Res 60: 5514–5521.

Kroemer A, Xiao X, Vu MD, Gao W, Minamimura K, Chen M *et al.* (2007). OX40 controls functionally different T cell subsets and their resistance to depletion therapy. J Immunol 179: 5584–5591.

Margolles-Clark E, Jacques-Silva MC, Ganesan L, Umland O, Kenyon NS, Ricordi C *et al.* (2009a). Suramin inhibits the CD40-CD154 costimulatory interaction: a possible mechanism for immunosuppressive effects. Biochem Pharmacol 77: 1236–1245.

Margolles-Clark E, Umland O, Kenyon NS, Ricordi C, Buchwald P (2009b). Small molecule costimulatory blockade: organic dye inhibitors of the CD40-CD154 interaction. J Mol Med 87: 1133–1143.

Margolles-Clark E, Kenyon NS, Ricordi C, Buchwald P (2010). Effective and specific inhibition of the CD40-CD154 costimulatory interaction by a naphthalenesulphonic acid derivative. Chem Biol Drug Des 76: 305–313.

Milroy LG, Brunsveld L, Ottmann C (2013). Stabilization and inhibition of protein-protein interactions: the 14-3-3 case study. ACS Chem Biol 8: 27–35.

Ottmann C (2013). Small-molecule modulators of 14-3-3 protein-protein interactions. Bioorg Med Chem 21: 4058–4062.

Pakala SV, Bansal-Pakala P, Halteman BS, Croft M (2004). Prevention of diabetes in NOD mice at a late stage by targeting OX40/OX40 ligand interactions. Eur J Immunol 34: 3039–3046.

Pawson AJ, Sharman JL, Benson HE, Faccenda E, Alexander SP, Buneman OP, Davenport AP, McGrath JC, Peters JA, Southan C, Spedding M, Yu W, Harmar AJ; NC-IUPHAR. (2014). The IUPHAR/BPS Guide to PHARMACOLOGY: an expert-driven knowledgebase of drug targets and their ligands. Nucl. Acids Res 42 (Database Issue): D1098–106.

Piconese S, Valzasina B, Colombo MP (2008). OX40 triggering blocks suppression by regulatory T cells and facilitates tumor rejection. J Exp Med 205: 825–839.

Redmond WL, Ruby CE, Weinberg AD (2009). The role of OX40-mediated co-stimulation in T-cell activation and survival. Crit Rev Immunol 29: 187–201.

Rose R, Erdmann S, Bovens S, Wolf A, Rose M, Hennig S *et al.* (2010). Identification and structure of small-molecule stabilizers of 14-3-3 protein-protein interactions. Angew Chem Int Ed Engl 49: 4129–4132.

Ruby CE, Yates MA, Hirschhorn-Cymerman D, Chlebeck P, Wolchok JD, Houghton AN *et al.* (2009). Cutting edge: OX40 agonists can drive regulatory T cell expansion if the cytokine milieu is right. J Immunol 183: 4853–4857.

Sheridan C (2013). Industry pursues co-stimulatory receptor immunomodulators to treat cancer. Nat Biotechnol 31: 181–183.

Silvian LF, Friedman JE, Strauch K, Cachero TG, Day ES, Qian F *et al.* (2011). Small molecule inhibition of the TNF family cytokine CD40 ligand through a subunit fracture mechanism. ACS Chem Biol 6: 636–647.

Smith RD, Hu L, Falkner JA, Benson ML, Nerothin JP, Carlson HA (2006). Exploring protein-ligand recognition with binding MOAD. J Mol Graph Model 24: 414–425.

So T, Croft M (2007). Cutting edge: OX40 inhibits TGF-beta- and antigen-driven conversion of naive CD4 T cells into $CD25^+$ $Foxp3^+$ T cells. J Immunol 179: 1427–1430.

Sugamura K, Ishii N, Weinberg AD (2004). Therapeutic targeting of the effector T-cell co-stimulatory molecule OX40. Nat Rev Immunol 4: 420–431.

Takeda I, Ine S, Killeen N, Ndhlovu LC, Murata K, Satomi S *et al.* (2004). Distinct roles for the OX40-OX40 ligand interaction in regulatory and nonregulatory T cells. J Immunol 172: 3580–3589.

Tansey MG, Szymkowski DE (2009). The TNF superfamily in 2009: new pathways, new indications, and new drugs. Drug Discov Today 14: 1082–1088.

Valzasina B, Guiducci C, Dislich H, Killeen N, Weinberg AD, Colombo MP (2005). Triggering of OX40 (CD134) on $CD4^{(+)}CD25^+$ T cells blocks their inhibitory activity: a novel regulatory role for OX40 and its comparison with GITR. Blood 105: 2845–2851.

Vu MD, Xiao X, Gao W, Degauque N, Chen M, Kroemer A *et al.* (2007). OX40 costimulation turns off $Foxp3^+$ Tregs. Blood 110: 2501–2510.

Wang G, Wang X, Yu H, Wei S, Williams N, Holmes DL *et al.* (2013). Small-molecule activation of the TRAIL receptor DR5 in human cancer cells. Nat Chem Biol 9: 84–89.

Weinberg AD, Rivera MM, Prell R, Morris A, Ramstad T, Vetto JT *et al.* (2000). Engagement of the OX-40 receptor *in vivo* enhances antitumor immunity. J Immunol 164: 2160–2169.

Weinberg AD, Morris NP, Kovacsovics-Bankowski M, Urba WJ, Curti BD (2011). Science gone translational: the OX40 agonist story. Immunol Rev 244: 218–231.

Wells JA, McClendon CL (2007). Reaching for high-hanging fruit in drug discovery at protein-protein interfaces. Nature 450: 1001–1009.

Whitty A, Kumaravel G (2006). Between a rock and a hard place? Nat Chem Biol 2: 112–118.

Xiao X, Balasubramanian S, Liu W, Chu X, Wang H, Taparowsky EJ *et al.* (2012). OX40 signaling favors the induction of T(H)9 cells and airway inflammation. Nat Immunol 13: 981–990.

Yao S, Zhu Y, Chen L (2013). Advances in targeting cell surface signalling molecules for immune modulation. Nat Rev Drug Discov 12: 130–146.

Supporting information

Additional Supporting Information may be found in the online version of this article at the publisher's web-site:

http://dx.doi.org/10.1111/bph.12819

Figure S1 Cell toxicities of the present compounds (**1**–**4**) assessed by a standard proliferation assay (BrdU) in THP-1 cells.

Figure S2 Cell toxicities of the present compounds (**1**–**4** plus tartrazine, TZ, as a negative control and erythrosine B, ErB, as a positive control) assessed by standard apoptosis assay (DAPI exclusion analysed by flow cytometry) in THP-1 cells.

Figure S3 Schild analysis of the interference with the OX40-OX40L binding activity for compound **4** (CVN).

Figure S4 Concentration dependence of the ligand-induced activation in CD40- and OX40-expressing NF-κB reporter sensor cells used in the present work.

Figure S5 Confirmation of activity for the present compounds of interest in OX40-expressing NF-κB reporter sensor cells.

Appendix S1 Quantification of receptor activation for competitive partial agonists in the presence of a full agonist using the minimal two-state receptor model.